

Abstract

A great need exists for reliable nighttime aerosol products at high spatial and temporal resolution. In this concept demonstration study, using Visible/Infrared Imager/Radiometer Suite (VIIRS) Day/Night Band (DNB) observations on the Suomi National Polar-orbiting Partnership (NPP) satellite, a new method is proposed for retrieving nighttime aerosol optical depth (τ) using the contrast between regions with and without artificial surface lights. Evaluation of the retrieved τ values against daytime AERONET data from before and after the overpass of the VIIRS satellite over the Cape Verde, Grand Forks, and Alta Floresta AERONET stations yields a coefficient of determination (r^2) of 0.71. This study suggests that the VIIRS DNB has the potential to provide useful nighttime aerosol detection and property retrievals.

1 Introduction

Recent advances in aerosol climate studies (e.g., Kaufman et al., 2002; Zhang et al., 2005a,b) and aerosol and visibility forecasting (e.g., Zhang et al., 2008a, 2011; Benedetti et al., 2009; Sekiyama et al., 2010) have responded to the growing demand for nighttime aerosol retrievals from satellite observations. For example, by using multi-sensor aerosol products from the MODerate-resolution Imaging Spectroradiometer (MODIS), the Multi-angle Imaging Spectroradiometer (MISR), and the Cloud Aerosol Lidar with Orthogonal Polarization (CALIOP), Zhang et al. (2011) show improvements in aerosol forecasts using combined 2-D/3-DVAR aerosol assimilation. Their study shows that higher forecast errors, measured by comparing modeled and AERONET aerosol optical depth (τ) data, occur at the 12 and 36 h forecast ranges, possibly due in part to a lack of nighttime observations. Similarly, reliable nighttime aerosol measurements would improve our understanding of the complete role of aerosol in the climate feedback system (e.g., Zhang et al., 2008b, 2003). Even if the efficacy of such a product was not as great as its daytime counterpart, provided the uncertainty is known,

AMTD

6, 587–612, 2013

Preliminary investigations toward aerosol optical depth retrievals

R. S. Johnson et al.

Title Page

Abstract

Introduction

Conclusions

References

Tables

Figures

⏪

⏩

◀

▶

Back

Close

Full Screen / Esc

Printer-friendly Version

Interactive Discussion

there is still a potential benefit for aerosol data assimilation applications (Reid et al., 2011).

Despite the increasing needs for aerosol information, the research community faces difficulty in finding nighttime satellite aerosol products that have wide spatial coverage and are optimized to their applications. For example, whereas the CALIOP lidar measures aerosol vertical distributions during both day and night in great detail, the spatial coverage of these data are limited because the instrument observes only a 2-D “curtain” through the atmosphere, with spacing of several hundred kilometers between orbital tracks. Furthermore, large uncertainties exist in converting CALIOP measurements of attenuated backscatter to physical quantities such as aerosol optical depth (e.g., Campbell et al., 2010; Winker et al., 2009). Lee et al. (2012) demonstrate the utility of thermal infrared (IR) channels in retrieving nighttime aerosol properties; however, such algorithms are only capable of detecting coarse mode aerosols, and the performance of these retrieval methods could degrade when dust plumes are near the surface.

Using nighttime observations in the visible/near infrared spectrum from the Operational Linescan System (OLS), Zhang et al. (2008b) demonstrate the potential of detecting aerosol plumes by examining the attenuation of artificial lights at night. However, the results from that study are qualitative as the OLS sensor lacks onboard calibrations. The recently launched Visible/Infrared Imager/Radiometer Suite (VIIRS) on the Suomi National Polar-orbiting Partnership (NPP) satellite also includes a Day/Night Band (DNB) low-light visible sensor that improves upon the OLS design. Unlike the OLS, the VIIRS DNB is well calibrated (e.g., Lee et al., 2006). In this study, we use VIIRS DNB observations to detect and retrieve the properties of nighttime aerosol using data from regions with and without artificial light emissions.

To use the VIIRS DNB sensor to retrieve nighttime τ we make several basic assumptions. First, we assume that the emission intensity of artificial light sources can be estimated and that a given artificial (city) light source is relatively stable throughout the study period. These assumptions highlight a need to carefully study the global

Preliminary investigations toward aerosol optical depth retrievals

R. S. Johnson et al.

Title Page

Abstract

Introduction

Conclusions

References

Tables

Figures



Back

Close

Full Screen / Esc

Printer-friendly Version

Interactive Discussion



under development and could be used in the future (e.g., Lanciano and Fiocco, 2007; Berkoff et al., 2011), but they are currently unavailable for this study period. Some extinction measuring lidars may be usable for our study, but currently we are unaware of any quality assured datasets available in our areas of interest.

Based on data availability, AERONET observations in closest temporal adjacency (before and after) to the VIIRS nighttime overpass were used for validation. Any before- and after-overpass AERONET data that were spaced more than 24 h apart from each other were not used in the study. The stations used were the Capo Verde station (16.7° N, 22.9° W – for validating retrievals from the city of Espargos on Sal Island), the Grand Forks station (47.9° N, 97.3° W – for validating retrievals from light sources near Grand Forks, North Dakota), and the Alta Floresta station (9.9° S, 56.1° W – for validating retrievals from the city of Alta Floresta, Brazil). The uncertainty in daytime AERONET τ values is roughly ± 0.015 (Schmid et al., 1999; Holben et al., 1998). The cloud screened level 1.5 AERONET data were used in this study as the level 2 AERONET data are not available for 2012 for the selected AERONET sites. Also, AERONET τ at 0.675 μm was used because the VIIRS DNB has a center wavelength of 0.7 μm with full-width at half-maximum response spectral range of 0.5 to 0.9 μm (e.g., Lee et al., 2006). AERONET and VIIRS data from 1 August to 31 October 2012 around Sal Island, from 11 June to 31 July 2012 for the Grand Forks area, and from 1 August to 30 September 2012 for Alta Floresta were used.

Three artificial light sources were chosen to represent dust (Cape Verde), urban-background (Grand Forks), and smoke (Alta Floresta) aerosol cases. These sites range from low and stable aerosol loading at Grand Forks to frequent high aerosol loading at Cape Verde and Alta Floresta. These AERONET sites were chosen to capture a wide range of aerosol patterns for the development of the retrieval discussed in this study. It should be noted that the purpose of this paper is not to develop a fully operational nighttime aerosol retrieval product, but to illustrate a new method of retrieving aerosol optical depth at night. Therefore, only limited study periods were used for the three illustrative test cases in this study.

**Preliminary
investigations toward
aerosol optical depth
retrievals**

R. S. Johnson et al.

Title Page

Abstract

Introduction

Conclusions

References

Tables

Figures

⏪

⏩

◀

▶

Back

Close

Full Screen / Esc

Printer-friendly Version

Interactive Discussion



3 Methodology and results

3.1 Method for estimating nighttime aerosol properties with VIIRS

Figure 1a shows nighttime VIIRS/DNB imagery of Sal Island on Cape Verde from 8 February 2012 at 03:45 UTC, where the AERONET data show τ of 1.6 on 7 February 2012 at 18:16 UTC and τ of 0.95 on 8 February 2012 at 10:47 UTC. In comparison, Fig. 1b shows nighttime VIIRS/DNB imagery from 9 February 2012 at 03:26 UTC, where the AERONET data show τ of 0.96 on 8 February 2012 at 18:08 UTC and 0.28 on 9 February 2012 at 13:32 UTC. The sharp reduction in τ over the course of the second night indicates a much reduced aerosol loading compared with the first night in Fig. 1a. Both Fig. 1a and b have similar observing conditions, with lunar zenith angles of 29.2° for 8 February and 17.0° for 9 February, and with moon fractions (100.0 = full moon) equal to 99.7 for 8 February and 97.9 for 9 February. The satellite zenith angle at the validation site for 8 February is 58.2° and is 38.0° for 9 February. In Fig. 1b, the land and ocean contrast can be detected, and artificial lights from the city of Espargos on Sal Island can be observed. Compared with the relatively low aerosol loading from Fig. 1b, the land and ocean contrast is almost completely obscured in Fig. 1a when aerosol loading is high. Also, the contrast between artificial city lights and the surrounding background is much reduced in Fig. 1a. Due to the aforementioned gain/offset noise problem, these February data are used only for illustrative purposes.

As suggested from Fig. 1, information from the VIIRS/DNB can be used to obtain nighttime aerosol physical properties because the contrast between artificial lights and nearby background radiances is reduced in the presence of aerosol plumes and clouds (i.e., via the horizontal diffusion of scattered artificial light). Utilizing this information, a method for retrieving τ can be developed.

This method is similar to the shadow method developed by Vincent et al. (2006) where the aerosol signals are detected by the difference between observed QuickBird radiance over shadow and non-shadow regions. Following Vincent et al. (2006), the

Preliminary investigations toward aerosol optical depth retrievals

R. S. Johnson et al.

Title Page

Abstract

Introduction

Conclusions

References

Tables

Figures



Back

Close

Full Screen / Esc

Printer-friendly Version

Interactive Discussion



surface upward radiance (I_s) from the combination of artificial and lunar light sources can be described as:

$$\pi I_s = r_s \left(\mu_0 F_0 e^{-\tau/\mu_0} + \mu_0 F_0 T(\mu_0) + \pi I_s \bar{r} \right) + \pi I_a \quad (1)$$

where r_s is the surface albedo (assuming a Lambertian surface), μ_0 is the cosine of the lunar zenith angle, F_0 is the incoming irradiance from the moon, τ is the total optical depth, $T(\mu_0)$ is the diffused transmittance for moonlight, \bar{r} is the aerosol reflectance, and I_a is the upwelling radiance from artificial light sources. Here we assume that I_a is an isotropic source, although a factor to correct for the angular dependence of I_a is applied in Eq. (7) below. The first and second terms on the right hand side of Eq. (1) represent the direct and diffused transmissions of moonlight. The third term represents the portion of upwelling surface radiance being reflected by the aerosol layer back to (and subsequently by) the surface, and the last term represents the direct emission from any artificial light sources present. By rearranging Eq. (1), we can solve for I_s as shown in Eq. (2).

$$I_s = \frac{r_s \left(\mu_0 F_0 e^{-\tau/\mu_0} + \mu_0 F_0 T(\mu_0) \right) + \pi I_a}{\pi (1 - r_s \bar{r})} \quad (2)$$

I_s represents the surface upward radiance, but to compute satellite observed radiance (I_{sat}), we need to consider the attenuation by the whole atmospheric column along the line-of-sight and diffuse transmission. Also, the path radiance (I_p), which represents the observed radiance of energy reflected and scattered by the atmosphere without ground interaction, is included.

$$I_{\text{sat}} = I_s e^{-\tau/\mu} + \mu I_s T(\mu) + I_p \quad (3)$$

Here μ is the cosine of the satellite viewing zenith angle, and τ is the total atmospheric column optical depth. In the visible spectrum, we assume τ is the optical depth from

Preliminary investigations toward aerosol optical depth retrievals

R. S. Johnson et al.

Title Page

Abstract

Introduction

Conclusions

References

Tables

Figures

◀

▶

◀

▶

Back

Close

Full Screen / Esc

Printer-friendly Version

Interactive Discussion



aerosol layers. Although, there will be some inherent uncertainty in this assumption since the DNB response function includes the oxygen A-band. A future study should consider the impact of the oxygen A-band on the proposed algorithm.

Similarly, for nearby background regions with no artificial light sources, Eq. (2) can be rewritten as

$$I'_s = \frac{r_s \left(\mu_0 F_0 e^{-\tau/\mu_0} + \mu_0 F_0 T(\mu_0) \right)}{\pi (1 - r_s \bar{r})}, \quad (4)$$

where I'_s is the surface upwelling radiance over nearby regions that have no artificial light sources and

$$I'_{\text{sat}} = I'_s e^{-\tau/\mu} + \mu I'_s T(\mu) + I_p, \quad (5)$$

I'_{sat} is the corresponding VIIRS radiance. By subtracting Eqs. (3) and (5) we get:

$$I_{\text{sat}} - I'_{\text{sat}} = \frac{I_a}{1 - r_s \bar{r}} \left(e^{-\tau/\mu} + \mu T(\mu) \right). \quad (6)$$

The first and second terms on the right hand side of Eq. (6) represent the direct and diffuse transmission of artificial light, respectively. For optically thin aerosol layers, the diffused part of the artificial light can be ignored. However, the diffused part could be significant for optically thick plumes. To account for the diffused radiance term, we introduce a correction term, k , which we assume is the ratio of direct to total (diffuse + direct) artificial light energy. Additionally, I_a needs to be estimated from a cloud, aerosol, and moon free sky. Because I_{sat} and I'_{sat} are by definition observed on a different night than the night from which I_a is derived, the satellite viewing geometry on these two nights could be different. For a single emission source, both I_a and I_{sat} are functions of satellite viewing zenith angle. Therefore, another correcting factor C (defined in Sect. 3.3) is introduced to account for differences in viewing geometries between the various nights.

Preliminary investigations toward aerosol optical depth retrievals

R. S. Johnson et al.

Title Page	
Abstract	Introduction
Conclusions	References
Tables	Figures
⏪	⏩
◀	▶
Back	Close
Full Screen / Esc	
Printer-friendly Version	
Interactive Discussion	



Also, note that $\bar{r} \sim 0.1$ for aerosol optical depth of 1 (e.g., Remer et al., 1998), so the term $r_s \bar{r}$ can be considered small and eliminated from Eq. (6) for low aerosol loading cases. The $r_s \bar{r}$ term, however, can be significant with thick aerosol plumes. For the study in this paper, we assume that the $r_s \bar{r}$ term can be ignored. Finally, we can calculate the aerosol optical depth as

$$\tau = -\mu \ln \left(\frac{k (I_{\text{sat}} - I'_{\text{sat}})}{C I_a} \right). \quad (7)$$

3.2 Distinguishing artificial lights from the background

As mentioned in Sect. 3.1, radiance values from both artificial light sources and the background are needed. Therefore, pixels containing direct artificial light emissions from Cape Verde, Grand Forks, and Alta Floresta need to be distinguished from the surrounding background pixels. For Grand Forks, identifying these direct artificial light pixels was accomplished by first focusing in on an area around the city (47.8° N to 48.05° N and 97.3° W to 96.9° W). All radiance values outside of this region were set to 0. Next the average of all the radiances within this region was calculated. Any pixel whose radiance exceeded 1.5 times the mean radiance, so long as the radiance was at least $0.5 \times 10^{-8} \text{ W cm}^{-2} \text{ sr}^{-1}$, was identified as a city pixel. A sample of nighttime imagery with and without the identified city pixels, highlighted in red, at Grand Forks can be seen in Fig. 1d and e. A sample of background radiances was also selected each night. For Grand Forks, a group of four pixels just north of the airport were manually chosen. An example of these pixels, highlighted in green, is shown in Fig. 1e.

To determine the representativeness of the background samples to the true background, two additional background samples were collected each night at Grand Forks. These extra samples can be seen, highlighted in yellow, in Fig. 1e. Each night, the absolute value of the relative error of each sample (using the three sample mean as truth) was calculated. The results of these calculations were averaged over the course of the study period for each sample, as shown in Table 1. The average absolute value

Preliminary investigations toward aerosol optical depth retrievals

R. S. Johnson et al.

Title Page

Abstract

Introduction

Conclusions

References

Tables

Figures

⏪

⏩

◀

▶

Back

Close

Full Screen / Esc

Printer-friendly Version

Interactive Discussion



of the relative error for the three samples over the course of the study period was approximately 0.06. For the retrieval described by Eq. (7), this results in an 11 % error at Grand Forks. For the calculation of retrieved τ discussed in the rest of this paper, the primary background samples, highlighted green in Fig. 1e, are used.

5 A different approach to choosing city pixels at Cape Verde was required because Espargos was the most consistently viewable city at this location. Thus, to ensure that only pixels from Espargos were selected, a group of 12 pixels containing the city were manually chosen. Of these 12 pixels, the six brightest pixels were selected as the city pixels for Cape Verde. A sample of the Cape Verde imagery with the group of
10 12 pixels, highlighted in red, can be seen in Fig. 1c. A group of 8 pixels just north of the city of Espargos was manually chosen each night to serve as the background sample. Imagery with these surrounding background pixels, highlighted in green, for Cape Verde is shown in Fig. 1c.

Similarly, Fig. 2a shows the nighttime VIIRS DNB image for Alta Floresta, Brazil on
15 3 August 2012. The artificial light source selection method that was used in the Cape Verde case was also applied to Alta Floresta. Each night, a block of 20×15 pixels covering Alta Floresta was chosen. Of these, the fifty brightest pixels, a sample of which is highlighted red in Fig. 2b, were selected to represent Alta Floresta. Similar to Fig. 1, the green pixels highlighted in Fig. 2b represent the background sample that
20 was manually chosen each night.

3.3 Derived parameters for the retrieval process

To derive aerosol optical depth via the method outlined in Eq. (7), values for I_a , C , and k are needed. The I_a values are considered to be emissions from artificial lights. As a first order approximation, we chose a radiance value for each city from a moonless
25 night where the pair of temporally nearest AERONET τ values from the previous and following days was at a minimum over a 24 h temporal window.

C is the correction factor compensating for the non-homogeneity property of artificial light intensity that is a function of satellite viewing zenith angle. As mentioned, we use

Preliminary investigations toward aerosol optical depth retrievals

R. S. Johnson et al.

Title Page

Abstract

Introduction

Conclusions

References

Tables

Figures



Back

Close

Full Screen / Esc

Printer-friendly Version

Interactive Discussion



Preliminary investigations toward aerosol optical depth retrievals

R. S. Johnson et al.

Title Page

Abstract

Introduction

Conclusions

References

Tables

Figures

⏪

⏩

◀

▶

Back

Close

Full Screen / Esc

Printer-friendly Version

Interactive Discussion



a value of I_{sat} from a moonless night with low aerosol loading to estimate I_a . For a given emission source however, I_a could be a function of viewing angle. Because of this potential dependence on viewing angle, we need C to account for the differences in viewing geometry between the night I_a is estimated and the other nights when I_{sat} is observed. Furthermore, C is also used to correct for an apparent change in I_a due to instrumental variations of radiance based on the satellite viewing zenith angle. Thus, to determine the value of C , the relationship between observed radiance and satellite viewing zenith angle needs to be investigated.

Figure 3a shows the relationship between observed radiance values (I_{sat}) from Grand Forks as a function of the cosine of the satellite viewing zenith angle (CVZA). A highly linear trend with a coefficient of determination (r^2) of 0.84 is found. Also, an approximately 30% decrease in radiance values are observed as CVZA goes from 0.5 to 1.0. The strong linear trend between radiance values from artificial light sources and CVZA from the Grand Forks study region shows the importance of this relationship and the need for the adjustment factor C .

It should be noted that the Grand Forks data used in this study is impacted by a known stray light issue that affects the VIIRS DNB sensor during high latitude summers. Currently, corrections for the stray light issue have not been implemented with the VIIRS data. The maximum possible impact of this stray light issue could only be on the same order of magnitude as the observed background sample values (I'_{sat}). However, the I'_{sat} values are an order of magnitude smaller than the I_{sat} values shown in Fig. 3a. Furthermore, the difference between the maximum and minimum I_{sat} values in Fig. 3a is larger than any of the I'_{sat} values. Thus, the stray light issue likely does not fully explain the trend seen in Fig. 3a. The impact of the stray light issue on this study is further suppressed by the fact that subtracting I_{sat} and I'_{sat} in Eq. (7) should cancel out this effect in the numerator of the equation. As for I_a in the denominator: at Grand Forks its value is an order of magnitude larger than the I'_{sat} values, and in Sect. 4.2 we show that this will introduce a maximum possible uncertainty in τ of 0.05–0.1 depending on CVZA.

Drawing from the results in Fig. 3a, it is possible to describe the dependence of radiance on the satellite zenith angle. This linear regression relationship can be described as follows:

$$I = -2.2249 \times 10^{-8} \times \cos(\theta) + 4.9808 \times 10^{-8} \quad (\text{Grand Forks}) \quad (8)$$

where I is the estimated radiance in $\text{W cm}^{-2} \text{sr}^{-1}$ and θ is the satellite zenith angle. The correction factor C is thus obtained by calculating I with the observing night viewing conditions and dividing it by the I that is calculated with the same viewing conditions as were present during the night which I_a was obtained.

$$C = \frac{I(\theta_{\text{sat}})}{I(\theta_{\text{Ia}})} \quad (9)$$

Figure 3b shows the observed radiance values from Cape Verde and Alta Floresta as a function of CVZA. No relationship (near zero correlation) is found between these two variables at either location. Therefore, C is set to 1 for the Cape Verde and Alta Floresta cases.

The k value represents the ratio of direct to total artificial light energy observed with the VIIRS DNB. We assume that, for a given atmospheric layer, the upward direct and diffuse transmittances equal the downward direct and diffuse transmittances, per the reciprocity principle. Based on this assumption and using the 6S radiative transfer model (Vermote et al., 1997), we estimate the k values. For the purpose of concept demonstration, we used an existing desert aerosol model (Vermote et al., 1997) in the 6S model to represent the Cape Verde cases, an urban aerosol model (Vermote et al., 1997) for the Grand Forks cases, and a biomass burning aerosol model (Vermote et al., 1997) for the Alta Floresta cases. No gaseous absorption is considered and the solar zenith angle is set to 0° . The ratios of direct to total downward solar radiation at the surface in the peak $0.7 \mu\text{m}$ spectral range were computed for 19 τ values (0, 0.05,

Preliminary investigations toward aerosol optical depth retrievals

R. S. Johnson et al.

Title Page

Abstract

Introduction

Conclusions

References

Tables

Figures

◀

▶

◀

▶

Back

Close

Full Screen / Esc

Printer-friendly Version

Interactive Discussion



0.1, 0.15, 0.2, 0.25, 0.3, 0.35, 0.4, 0.45, 0.5, 0.55, 0.6, 0.7, 0.8, 0.9, 1.0, 1.2, and 1.5) and were used as the k values. To simplify the calculation, we assumed a solution at the VIIRS DNB peak wavelength. However, follow-up studies are needed to carefully evaluate k values with the use of the actual sensor filter function and artificial light emission spectrum.

4 Assessment

4.1 Results

Figure 4a shows the comparison between the τ derived from Eq. (7) and AERONET derived τ . Mean values of two bracketing AERONET observations (defined as the most recent daytime measurement from before the VIIRS nighttime overpass and the first measurement after the overpass the following day, so long as the two measurements are no more than 24 h apart), are used to represent the nighttime AERONET value. The error bars of the AERONET data represent the τ range between the two daytime AERONET values that are used for estimating the nighttime value. As seen in Table 2 and Fig. 4a, the coefficient of determination of the estimated nighttime AERONET τ and τ derived from Eq. (7) (with $k = 1$) is 0.69 (RMSE of 0.14). However, a systematic low bias in the VIIRS-retrieved τ is also observed for the data from Cape Verde. The low bias is likely due to the upward diffuse transmission term in Eq. (7) that is not accounted for when k is equal to 1. Figure 4b shows the same comparison with k values calculated as mentioned previously, using the urban aerosol model for Grand Forks, the desert aerosol model for Cape Verde, and the biomass burning aerosol model for Alta Floresta. With the diffuse transmission term taken into account, the underestimation of τ improves and a closer to one-to-one relationship between AERONET and VIIRS τ is found. Table 2 shows the coefficient of determination, slope, and RMSE values for two cases: (1) the upward diffuse transmission term was not taken into account by setting k to one, and (2) k values were estimated using the desert aerosol model

**Preliminary
investigations toward
aerosol optical depth
retrievals**

R. S. Johnson et al.

Title Page

Abstract

Introduction

Conclusions

References

Tables

Figures

⏪

⏩

◀

▶

Back

Close

Full Screen / Esc

Printer-friendly Version

Interactive Discussion

for Cape Verde, the urban aerosol model for Grand Forks, and the biomass burning aerosol model for Alta Floresta. Table 2 suggests that the retrieved τ is sensitive to the aerosol model used in the retrieval process.

Figure 4 suggests that Eq. (7) may be viable for estimating nighttime aerosol optical depth from VIIRS. However, a careful selection of target artificial light sources, and a careful study of C , k , and the stability of I_a are needed before applying the algorithm to a larger domain.

Figure 5 shows a time series of Level 1.5 AERONET τ and the retrieved VIIRS nighttime τ based on Eq. (7). The retrieved nighttime τ values generally follow the AERONET τ . At Grand Forks (Fig. 5a), VIIRS τ retrievals were less than zero for two nights, and these retrievals were set to zero. However, when the urban aerosol model was used to estimate k values, these retrievals were both positive. Several negative retrievals at Alta Floresta (Fig. 5c) were also obtained and set to zero. These retrievals are likely due to the estimated value for I_a . Correcting for the diffuse transmission of artificial light appears to improve the performance of the VIIRS retrieved τ at Cape Verde (Fig. 5b), especially for high aerosol loading cases. At the beginning of the time series for Alta Floresta (Fig. 5c), the AERONET τ values are low, increasing to 0.4–0.5 by the end of August and remaining at elevated levels into September. A similar pattern is also captured by the retrieved nighttime τ from VIIRS.

There are a few limitations in this study. First, in the derivation of Eq. (7), it was assumed that the quantity $r_s \bar{r}$ is negligible. However, this assumption will begin to break down as the amount of aerosol in the atmospheric column increases. Thus, due to this assumption alone, one would expect that the proposed algorithm will perform worse for high τ cases without any further modifications. Compounding the problem of the $r_s \bar{r}$ assumption is the fact that the signal to background ratio at Cape Verde is not particularly strong, especially on nights with moonlight. The low signal to background ratio at Cape Verde, especially on nights with high τ , might introduce difficulty in obtaining an accurate signal for retrieving τ . Thus, using cities with higher signal to background ratios (brighter lights), such as Grand Forks, is more ideal.

**Preliminary
investigations toward
aerosol optical depth
retrievals**

R. S. Johnson et al.

Title Page

Abstract

Introduction

Conclusions

References

Tables

Figures



Back

Close

Full Screen / Esc

Printer-friendly Version

Interactive Discussion



4.2 Sensitivity of the retrieved process to I_a , C , and k

Being important components of the retrieval process, it is necessary to estimate the sensitivity of the retrieval process to errors in I_a , C , and k . The uncertainty in retrieved τ can be written by taking the total derivative of Eq. (7):

$$d\tau = \mu \left(\frac{dI_a}{I_a} - \frac{d\Delta I}{\Delta I} + \frac{dC}{C} - \frac{dk}{k} \right), \quad (10)$$

where ΔI is $I_{\text{sat}} - I'_{\text{sat}}$. Each term on the right hand side of Eq. (10) represents the relative error of a quantity composing τ in Eq. (7). For example, a 5% change in C , or $dC/C = 0.05$, introduces an uncertainty in the retrieved τ of 0.05μ . This leads to an uncertainty in τ of 0.05 at nadir ($\mu = 1$) and 0.025 at a viewing angle of 60° ($\mu = 0.5$).

The uncertainty of retrieved τ , based on Eq. (10), is not a function of τ . Therefore, the larger τ is, the smaller the relative uncertainty of the retrieved τ . A 5% change in C at nadir introduces a 10% uncertainty for $\tau = 0.5$ and a 5% uncertainty for $\tau = 1$. The relative uncertainty in retrieved τ decreases as τ increases. The same is true regarding the satellite viewing angle; the relative uncertainty in τ decreases as the viewing angle increases. Based on Eq. (10), similar arguments also hold for I_a , ΔI , and k . It is interesting to note the various components of uncertainty in Eq. (10) may partially cancel each other. For instance, increasing uncertainties in C and k will decrease the total uncertainty in τ so long as the uncertainties are either both positive or both negative.

As alluded to earlier, Eq. (10) can also give us an estimate of the impact the VIIRS DNB stray light issue will have on the retrieved τ values at Grand Forks. As noted in Sect. 3.3, the maximum impact of the stray light issue would be on the same order of magnitude as the background values, which is an order of magnitude smaller than I_a , or approximately 10%. By Eq. (10), a 10% error in I_a will lead to a maximum uncertainty of 0.05 at a viewing angle of 60° ($\mu = 0.5$) and a maximum uncertainty of 0.1 at nadir.

Title Page

Abstract

Introduction

Conclusions

References

Tables

Figures

◀

▶

◀

▶

Back

Close

Full Screen / Esc

Printer-friendly Version

Interactive Discussion

5 Conclusions and implications

To demonstrate a new concept in this paper, a new method for retrieving the properties of nighttime aerosol using observations from the VIIRS DNB are presented. The new method is based on theoretical radiative transfer equations for the retrieval of aerosol optical depth using signal differences between areas with and without artificial light emissions. This study suggests:

1. The contrast between regions with and without artificial lights can be effectively used in retrieving aerosol optical depth, and this method deserves further evaluation as a potential operational satellite nighttime aerosol product.
2. The parameters, C and I_a are notable sources of uncertainty in the aerosol optical depth retrievals, and their sensitivity needs to be further evaluated in future studies. Also, determining the ratio of observed direct and total (direct + diffuse) artificial light energy, k , needs to be investigated for more accurate retrievals. Future work should include additional nighttime τ validation sources besides AERONET, such as CALIPSO.
3. Using artificial lights to obtain nighttime aerosol properties is feasible; however the temporal and geometric variations of artificial light source intensity needs to be studied in order to apply this technique globally.
4. Cloud detection, especially thin cirrus cloud detection, is important to the proposed aerosol retrieval method. Alternatively, the method illustrated in this study for aerosol property retrievals can be directly applied to nighttime cloud property retrievals.
5. Although not discussed in this paper, with the presence of aerosol plumes, the changes in TOA reflectance are clearly observable from the VIIRS DNB. This piece of information alone can be used to develop an aerosol product in a future study using similar approaches currently implemented in the daytime algorithms

Preliminary investigations toward aerosol optical depth retrievals

R. S. Johnson et al.

Title Page

Abstract

Introduction

Conclusions

References

Tables

Figures

⏪

⏩

◀

▶

Back

Close

Full Screen / Esc

Printer-friendly Version

Interactive Discussion



(e.g., Remer et al., 2005), taking advantage of a lunar model tailored to the VIIRS DNB (e.g., Miller and Turner, 2009).

Acknowledgements. This research was funded by the Office of Naval Research Code 32 and the UND seed money grant. Author S. D. M. acknowledges the support of the Naval Research Laboratory through contract N00173-10-C-2003. The group acknowledges the AERONET program, their contributing principal investigators and their staff for coordinating the sites used in this investigation.

References

- Benedetti, A., Morcrette, J.-J., Boucher, O., Dethof, A., Engelen, R. J., Fisher, M., Flentje, H., Huneeus, N., Jones, L., Kaiser, J. W., Kinne, S., Mangold, A., Razinger, M., Simmons, A. J., and Suttie, M.: Aerosol analysis and forecast in the European Centre for Medium-Range Weather Forecasts Integrated Forecast System: 2. Data assimilation, *J. Geophys. Res.*, 114, D13205, doi:10.1029/2008JD011115, 2009.
- Berkoff, T. A., Sorokin, M., Stone, T., Eck, T. F., Raymond Hoff, R., Welton, E., and Holben, B.: Nocturnal Aerosol Optical Depth Measurements with a Small-Aperture Automated Photometer Using the Moon as a Light Source, *J. Atmos. Ocean. Tech.*, 28, 1297–1306, 2011.
- Campbell, J. R., Reid, J. S., Westphal, D. L., Zhang, J., Hyer, E. J., and Welton, E. J.: CALIOP aerosol subset processing for global aerosol transport model data assimilation, *J. Sel. Top. Appl. Earth Obs.*, 3, 203–214, doi:10.1109/JSTARS.2010.2044868, 2010.
- Campbell, J. R., Tackett, J. L., Reid, J. S., Zhang, J., Curtis, C. A., Hyer, E. J., Sessions, W. R., Westphal, D. L., Prospero, J. M., Welton, E. J., Omar, A. H., Vaughan, M. A., and Winker, D. M.: Evaluating nighttime CALIOP 0.532 μm aerosol optical depth and extinction coefficient retrievals, *Atmos. Meas. Tech.*, 5, 2143–2160, doi:10.5194/amt-5-2143-2012, 2012.
- Elvidge, C. D., Baugh, K. E., Dietz, J. B., Bland, T., Sutton, P. C., and Kroehl, H. W.: Radiance calibration of DMSP-OLS low-light imaging data of human settlements, *Remote Sens. Environ.*, 68, 77–88, 1999.
- Elvidge, C. D., Imhoff, M. L., Baugh, K. E., Hobson, V. R., Nelson, I., Safran, J., Dietz, J. B., and Tuttle, B. T.: Night-time lights of the world: 1994–1995, *ISPRS J. Photogramm. Remote Sens.*, 56, 81–99, 2001.

Preliminary investigations toward aerosol optical depth retrievals

R. S. Johnson et al.

Title Page

Abstract

Introduction

Conclusions

References

Tables

Figures

⏪

⏩

◀

▶

Back

Close

Full Screen / Esc

Printer-friendly Version

Interactive Discussion



**Preliminary
investigations toward
aerosol optical depth
retrievals**

R. S. Johnson et al.

Title Page

Abstract

Introduction

Conclusions

References

Tables

Figures

⏪

⏩

◀

▶

Back

Close

Full Screen / Esc

Printer-friendly Version

Interactive Discussion



Winker, D. M., Vaughan, M. A., Omar, A., Hu, Y., Powell, K. A., Liu, Z., Hunt, W. H., and Young, S. A.: Overview of the CALIPSO Mission and CALIOP Data Processing Algorithms, *J. Atmos. Ocean. Tech.*, 26, 2310–2323, 2009.

Zhang, J. and Christopher, S. A.: Longwave radiative forcing of Saharan dust aerosols from Terra, *Geophys. Res. Lett.*, 30, 2188, doi:10.1029/2003GL018479, 2003.

Zhang, J., Christopher, S. A., Remer, L. A., and Kaufman, Y. J.: Shortwave aerosol radiative forcing over cloud-free oceans from Terra: 1. Angular models for aerosols, *J. Geophys. Res.*, 110, D10S23, doi:10.1029/2004JD005008, 2005a.

Zhang, J., Christopher, S. A., Remer, L. A., and Kaufman, Y. J.: Shortwave aerosol radiative forcing over cloud-free oceans from Terra: 2. Seasonal and global distributions, *J. Geophys. Res.*, 110, D10S24, doi:10.1029/2004JD005009, 2005b.

Zhang, J. Reid, J. S., Westphal, D. L., Baker, N. L., and Hyer, E. J.: A system for operational aerosol optical depth data assimilation over global oceans, *J. Geophys. Res.*, 113, D10208, doi:10.1029/2007JD009065, 2008a.

Zhang, J., Reid, J. S., Turk, J., and Miller, S.: Strategy for studying nocturnal aerosol optical depth using artificial lights, *Int. J. Remote Sens.*, 29, 4599–4613, 2008b.

Zhang, J., Campbell, J. R., Reid, J. S., Westphal, D. L., Baker, N. L., Campbell, W. F., and Hyer, E. J.: Evaluating the impact of assimilating CALIOP-derived aerosol extinction profiles on a global mass transport model, *Geophys. Res. Lett.*, 38, L14801, doi:10.1029/2011GL047737, 2011.

**Preliminary
investigations toward
aerosol optical depth
retrievals**

R. S. Johnson et al.

Table 1. Average absolute relative error values for different background samples from Grand Forks, using the nightly sample mean as truth.

	Sample 1 Grand Forks	Sample 2 Grand Forks	Sample 3 Grand Forks
Average absolute relative error	0.066	0.038	0.062

Title Page

Abstract

Introduction

Conclusions

References

Tables

Figures

⏪

⏩

◀

▶

Back

Close

Full Screen / Esc

Printer-friendly Version

Interactive Discussion



Preliminary investigations toward aerosol optical depth retrievals

R. S. Johnson et al.

Table 2. Coefficient of Determination, Slope, and RMSE values obtained by comparing the retrievals from Eq. (7) to average AERONET τ values taken from before and after the VIIRS satellite overpass. Results are shown for the case where no diffuse transmission correction is applied (k in Eq. 7 set to 1), and the case where the 6s urban aerosol model is used for Grand Forks, the desert model is used for Cape Verde, and the biomass burning model is used for Alta Floresta.

	Coefficient of determination	Slope	RMSE
Retrieved τ (no diffuse transmission correction)	0.69	0.60	0.14
Retrieved τ (with diffuse transmission correction)	0.71	0.91	0.12

[Title Page](#)
[Abstract](#)
[Introduction](#)
[Conclusions](#)
[References](#)
[Tables](#)
[Figures](#)
[⏪](#)
[⏩](#)
[◀](#)
[▶](#)
[Back](#)
[Close](#)
[Full Screen / Esc](#)
[Printer-friendly Version](#)
[Interactive Discussion](#)

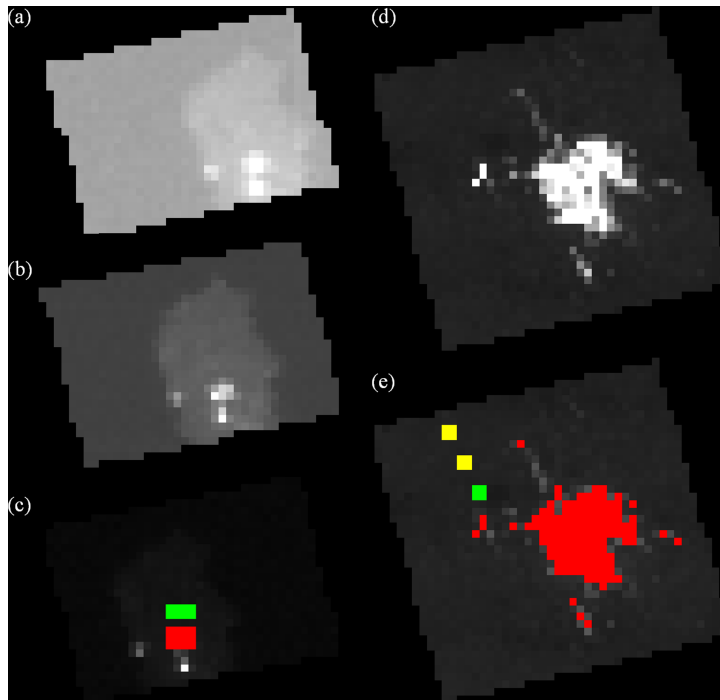



Fig. 1. (a) VIIRS nighttime imagery over Sal Island from the VIIRS Day/Night Band for 8 February 2012. The island is less observable due to the presence of a heavy aerosol plume. (b) Similar to (a) but for a relatively low aerosol loading night of 9 February 2012. Sal Island can more easily be visually identified from the imagery. (c) Similar to (b) but 27 October 2012 and with the artificial light sources (manually identified) highlighted in red and selected background pixels highlighted in green. (d)–(e) Similar to (b)–(c) but for the Grand Forks region on 5 June 2012 and with artificial light sources algorithmically identified. Also, additional background samples are highlighted in yellow. Imagery is radiance ($\text{W cm}^{-2} \text{sr}^{-1}$) multiplied by 10^{10} and then plotted in grayscale with values ranging from 0 to 255, where any value over 255 was set to 255.

Preliminary investigations toward aerosol optical depth retrievals

R. S. Johnson et al.

Title Page

Abstract Introduction

Conclusions References

Tables Figures

⏪ ⏩

⏴ ⏵

Back Close

Full Screen / Esc

Printer-friendly Version

Interactive Discussion



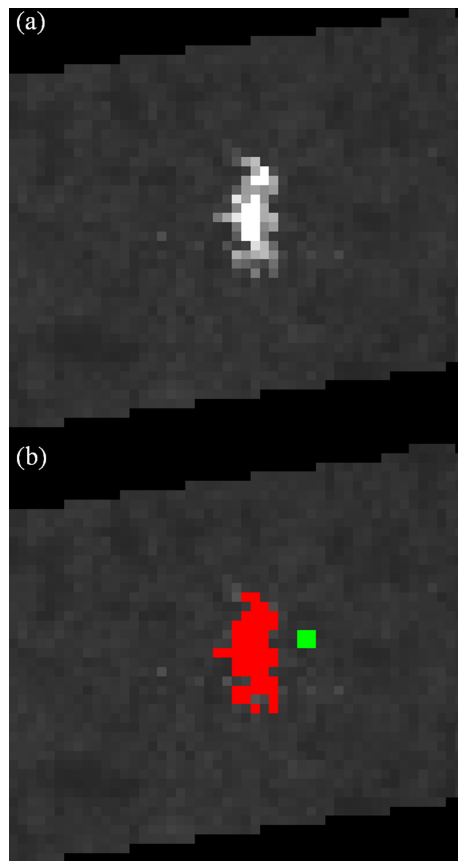


Fig. 2. (a) VIIRS nighttime imagery over Alta Floresta for 3 August 2012. (b) Similar to (a) with artificial city light sources highlighted in red (collection of the brightest pixels from a manually selected box of pixels covering the city) and manually selected background pixels highlighted in green.

Preliminary investigations toward aerosol optical depth retrievals

R. S. Johnson et al.

Title Page

Abstract

Introduction

Conclusions

References

Tables

Figures

◀

▶

◀

▶

Back

Close

Full Screen / Esc

Printer-friendly Version

Interactive Discussion

**Preliminary
investigations toward
aerosol optical depth
retrievals**

R. S. Johnson et al.

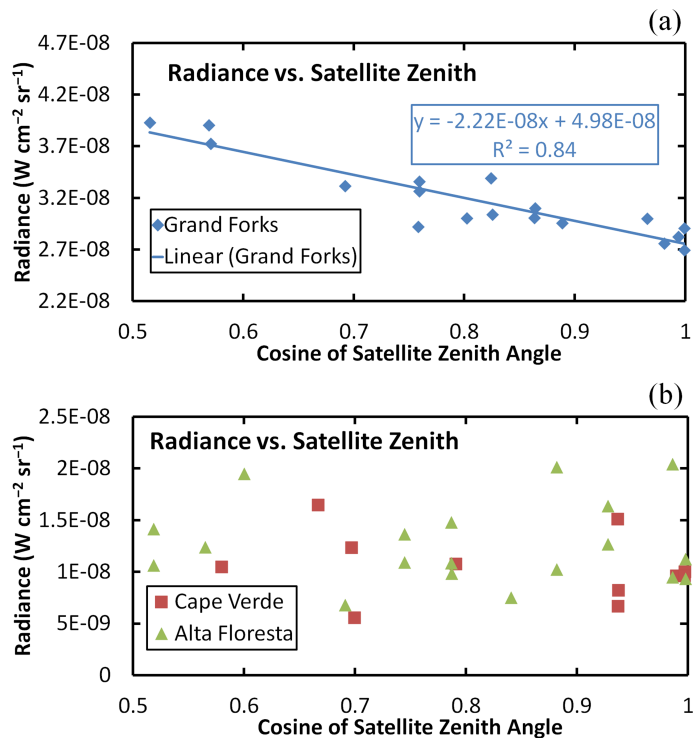


Fig. 3. (a) Radiance versus the cosine of the satellite viewing zenith angle for Grand Forks (blue). (b) Radiance versus the cosine of the satellite viewing zenith angle for Cape Verde (red) and Alta Floresta (green).

Title Page

Abstract

Introduction

Conclusions

References

Tables

Figures

◀

▶

◀

▶

Back

Close

Full Screen / Esc

Printer-friendly Version

Interactive Discussion

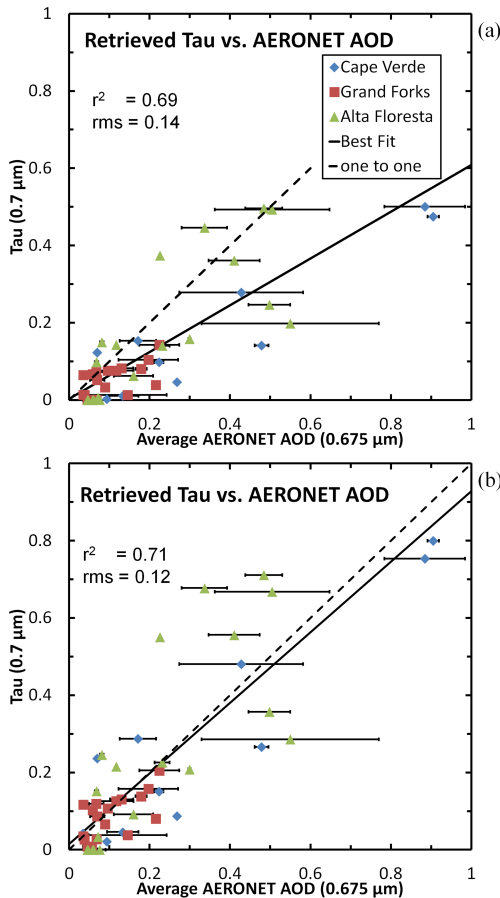


Fig. 4. (a) Scatter plot of estimated AERONET τ (approximated by the nearest daytime observations) versus VIIRS retrieved τ ignoring the diffuse transmission of artificial light ($k = 1$), and (b) for k estimated with the 6S model using the urban aerosol model for Grand Forks, the desert aerosol model for Cape Verde, and the biomass burning aerosol model for Alta Floresta.

**Preliminary
investigations toward
aerosol optical depth
retrievals**R. S. Johnson et al.

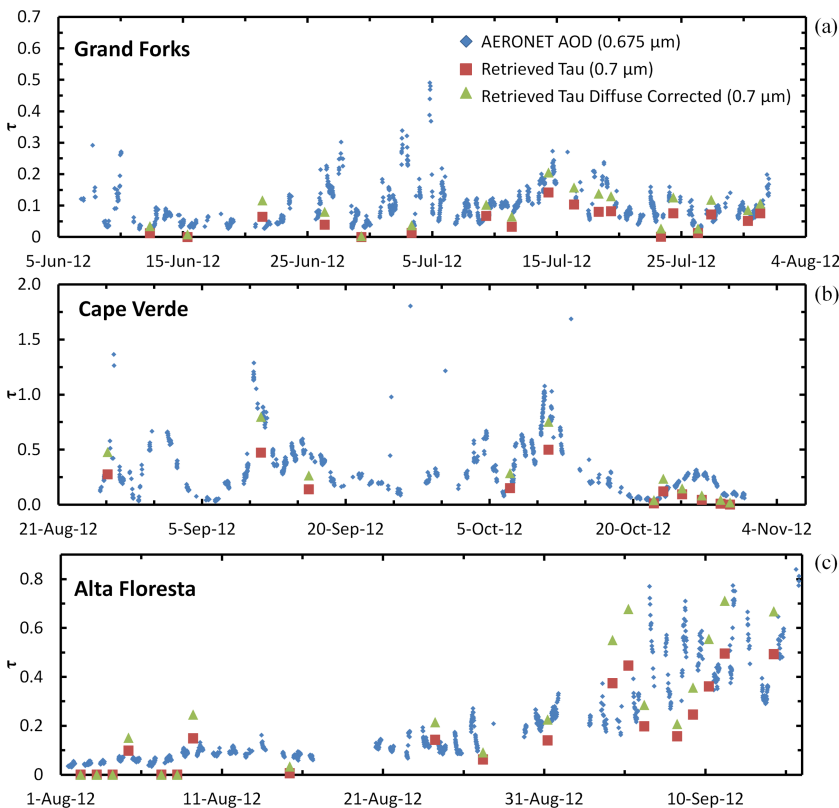


Fig. 5. (a) Time series for Grand Forks showing AERONET τ , and VIIRS retrieved τ ignoring the diffuse transmission of light ($k = 1$) and using the 6S urban aerosol model to estimate k . (b) Similar to (a) except for Cape Verde and using the 6S desert aerosol model to estimate k . (c) Similar to (a) except for Alta Floresta and using the 6S biomass burning aerosol model to estimate k .